minerals

MDPI

Article

Multi-Tool (LA-ICPMS, EMPA and XRD) Investigation on Heavy Minerals from Selected Holocene Peat-Bog Deposits from the Upper Vistula River Valley, Poland

Krzysztof Szopa [1,*], Sylwia Skreczko [1], David Chew [2], Tomasz Krzykawski [1] and Artur Szymczyk [1]

[1] Faculty of Natural Sciences, Institute of Earth Sciences, University of Silesia in Katowice, Poland, Będzińska 60, 41-200 Sosnowiec, Poland; sylwia.skreczko@us.edu.pl (S.S.); tomasz.krzykawski@us.edu.pl (T.K.); artur.szymczyk@us.edu.pl (A.S.)

[2] Department of Geology, School of Natural Sciences, Trinity College Dublin, Dublin 2, Ireland; chewd@tcd.ie

* Correspondence: krzysztof.szopa@us.edu.pl; Tel.: +48-603-813-074

Received: 8 November 2019; Accepted: 16 December 2019; Published: 20 December 2019

Abstract: Peat sediments represent important environmental and climatic archives, as well as recording information on the processes affecting the formation of these deposits; combined these data can be used for paleoreconstruction of peat-bogs. In this paper we characterize heavy mineral-rich sandy layers from two peat-bog sites in Mizerów and Strumień (Poland). In both cases, the most common identified mineral suite is: epidote, staurolite, tourmaline (dravite and schörl), garnet, spinel, Al_2SiO_5 polymorphs (sillimanite, kyanite, andalusite), amphibole (mainly hornblende), pyroxene (e.g., richterite, diopside), perovskite, topaz, cordierite, apatite, monazite, chromite, ilmenite, chlorite, iron oxides, rutile and siderite. This mineral suite is characteristic of a metamorphic aureole surrounding a magmatic body. Pyrite is likely authigenic in origin. Apatite and monazite were employed for U-Pb and CHIME dating, respectively. Based on the U-Pb age information composition and textural features of selected minerals, different provenance areas were indicated: the Tatra Massif, the Bohemian Massif, and the Silesian Basin area. Transport of the investigated mineral phases was linked to development of both the Odra (praOdra) and the Vistula valleys.

Keywords: heavy minerals; U-Pb dating; CHIME dating; peat; Upper Vistula River Valley

1. Introduction

Peat-bogs are the important components of temperate landscapes, which form under particular environmental conditions. Moreover, they are associated with specific vegetation types. Peat-bogs are regarded as archives of past vegetation changes associated with both the regional climate and the evolution of the local environment. This type of biogenic reservoir may be exposed to external factors, including periodic hydrological changes, fires, etc. When peat-bogs are frequently flooded, allochthonous sandy material may be delivered into the bog system. Another common process that can supply detritus is aeolian activity [1].

Analysis of heavy minerals in Quaternary sediments is used to determine local changes in transport direction e.g., [2,3], mode of sediment transport, as well as the depositional processes and the environment of accumulation [4–8]. For accurate interpretation of the heavy minerals present in Quaternary sediments, it is important to determine their resistance to chemical weathering and mechanical abrasion [9,10] due to the variable preservation of mineral grains [11–14].

For this study we used quantitative X-ray diffraction analysis, scanning electron microscope (SEM) imaging, electron microprobe analysis (EMPA), as well as apatite U-Pb dating. This methodology provides a multi-tool approach for understanding the composition of detrital heavy minerals in peat-bogs and is used to constrain their provenance area. Moreover, we present the first mineralogical investigation of peats located close to the "Moravian Gate" (Figure 1), which is located between the Carpathian Mountains range (the Tatra Massif) in the east and the Bohemian Massif (the Sudety Mountains) in the west. The selected area of study has never been investigated in terms of geochemistry, as well as paleobotany. The results of this study provide information on factors affecting the accumulation of peat, determining local changes in the type of the allochthonous material transport in the Upper Vistula Valley.

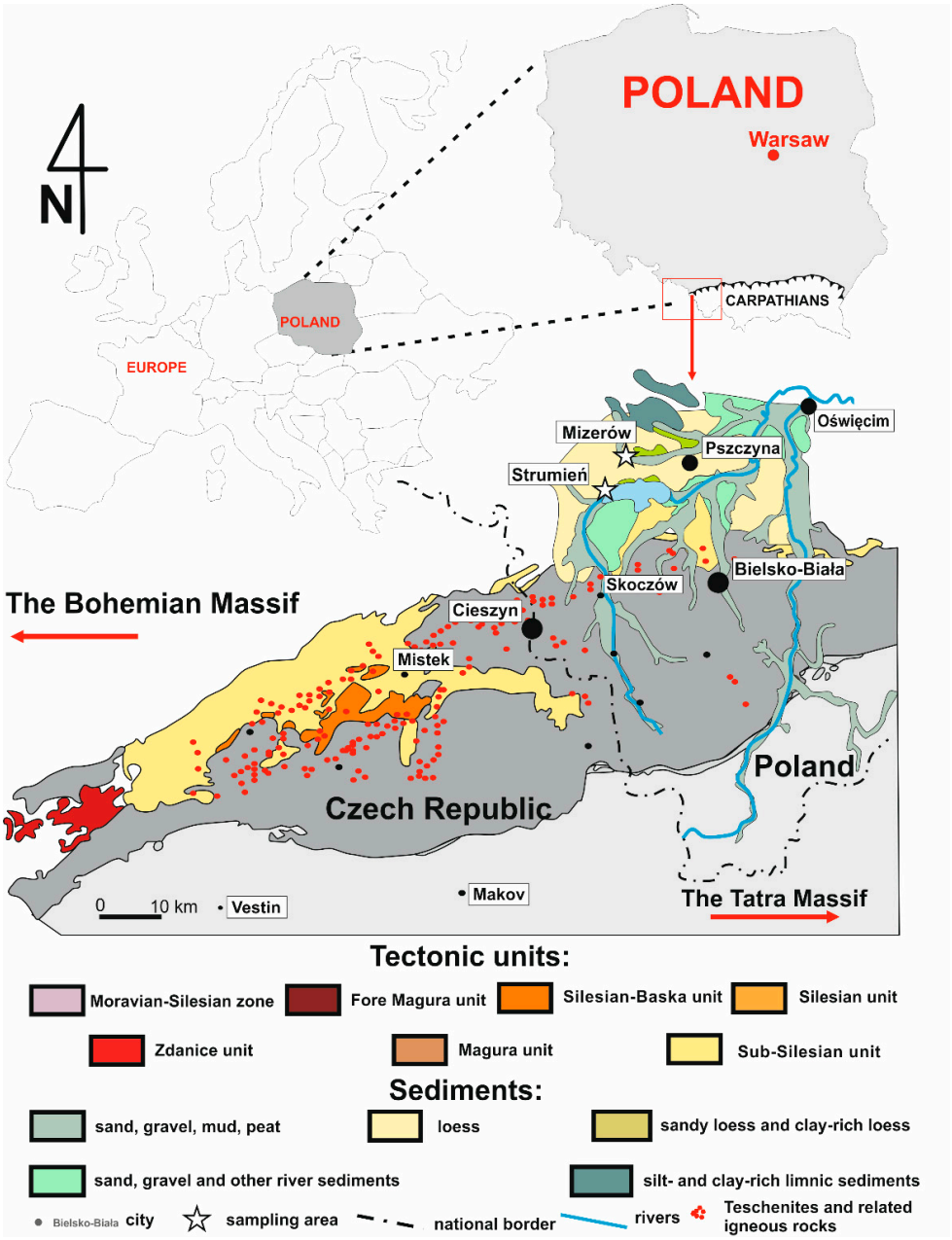

Figure 1. Simplified geological map of the tectonic elements of the Outer Western Carpathians based on Żytko et al. [15] with marked sampling areas. All magmatic rock localities (the teschenite-picrite association in the Silesian Basin) after Włodyka [16].

2. Materials and Methods

2.1. Geology

The Strumień and Mizerów peat-bogs are located in the Oświęcim Basin in the Upper Vistula River Valley [17] (Pszczyna County, Poland). The studied area belongs to the Fore-Carpathian Depression. The basement contains Carboniferous organic-rich sedimentary rocks, overlain by Miocene sediments (clays intercalated with sands). The youngest sediments comprise Quaternary fluvioglacial sands and gravels, river-profluvium sands and gravels, limnic-glacial sediments, peat (Holocene in age), which are locally overlain by sandy loess and loess-like sediments in the northern part of the study area (Figure 1; [18]). Quaternary glaciations (Odranian, Sanian 1, Sanian 2) [19] changed the flow of rivers, and also influenced the local depositional environments. In the study area, an alluvial fan occurs on the Vistula River. The Vistula River starts in the Carpathian Foothills, where it is up to 3–4 m deep and is up to 10 km wide. Its total fan length is 23 m [20,21]. Palynological analysis and radiocarbon dating suggest that the alluvial fan on the Vistula River and other Carpathian-derived rivers formed mainly in the Pleniglacial of the last glaciation, while the older proluvial remnants are preserved as residues [21]. Fossil peats (e.g., Drogomyśl, Chybie, Pierścieniec) occurring within the alluvial fan of the Vistula River represent interstadials yielding a wide range of ages from >45 ka BP to the early Holocene [22,23].

The Strumień peat-bog (N49°55′4″, E18°45′21″), is located in a pan-like valley in the northern part of the alluvial fan along the Vistula River (Figure 1). This region is surrounded by a flood plain. The Mizerów peat-bog (N49°59′44″, E18°48′32″) is located ~10 km north of the Strumień site, and formed within transgressive ice-dam lakes (Figure 1; [24]).

2.2. Peat Samples

Peat sampling was undertaken between August and October 2015 in two bogs (the Strumień and Mizerów sites). Sampling was performed with a Instorf-Eijkelkamp Ø 80 auger (Eijkelkamp Soil & Water, The Netherlands). The type of sediment and peat units were distinguished using Tolpa's classification [25,26]. The degree of peat decomposition was defined using the von Post scale [27].

The Strumień peat-bog has an area c. 0.9 ha, and is covered by wetland vegetation and sparse Alnus trees. The sampling profile was 1.20 m thick. In the upper part of the profile, a clay layer (0.00–0.20 m thick; Table S1) is present, with identified plant macro-remains (*Carex canescens*, *Carex nigra*, *Carex rostrata*, *Juncus* sp.; Table S2). Layers of sand were identified at 0.55–0.60 m and 0.95–1.00 m depth (Figure 2). In the Strumień peat-bog profile, mainly *Magnocaricioni/Carici* and *Magnocaricioni/Carici-Phragmitetii* peats were deposited in rush communities. In the interval 0.8–0.9 m, as a result of the change of vegetation in the bog, *Alnioni/Alneti* peat was deposited. Gyttja (mud formed from the partial decay of peat) was identified in the base interval of 1.00–1.20 m (Figure 2).

The Mizerów peat-bog covers an area of 136 ha, and is overgrown by wetland vegetation, and is partly surrounded by both forest and farmland. Clay-rich gyttja was noted in the upper part of the profile (0.00–0.60 m), with a zonation of plant macro-remains (Table S3). In the 0.00–0.30 m interval, the identified species (Table S4) include: *Alnus glutinosa*, *Carex* sp., *Drepanocladus* sp., *Phramites australis*, *Sambucus* sp., and *Urtica* sp. In the interval between 0.30 and 0.50 m, *Asteraceae* sp., *Nuphar pumila*, *Drepanocladus* sp., *Sambucus* sp. were distinguished. In the lower part of the gyttja horizon are plant macro-remains, *Nuphar pumila*, *Poaceae* sp. *Potamogeton natans*, *Schoenoplectus* sp. In the interval between 0.60 and 0.80 m, the layers of the gyttja pass downwards into peat up to a depth of 1.90 m. In the profile, three layers of sand were noted at 1.00–1.05 m and 1.50–1.55 m depth, as well as in the floor part of core (Figure 2). In the Mizerów peat-bog profile two types of peat were deposited: *Magnocaricioni/Carici-Phragmitetii* and *Magnocaricioni/Phragmitetii* peat, whose formation is related to rush vegetation.

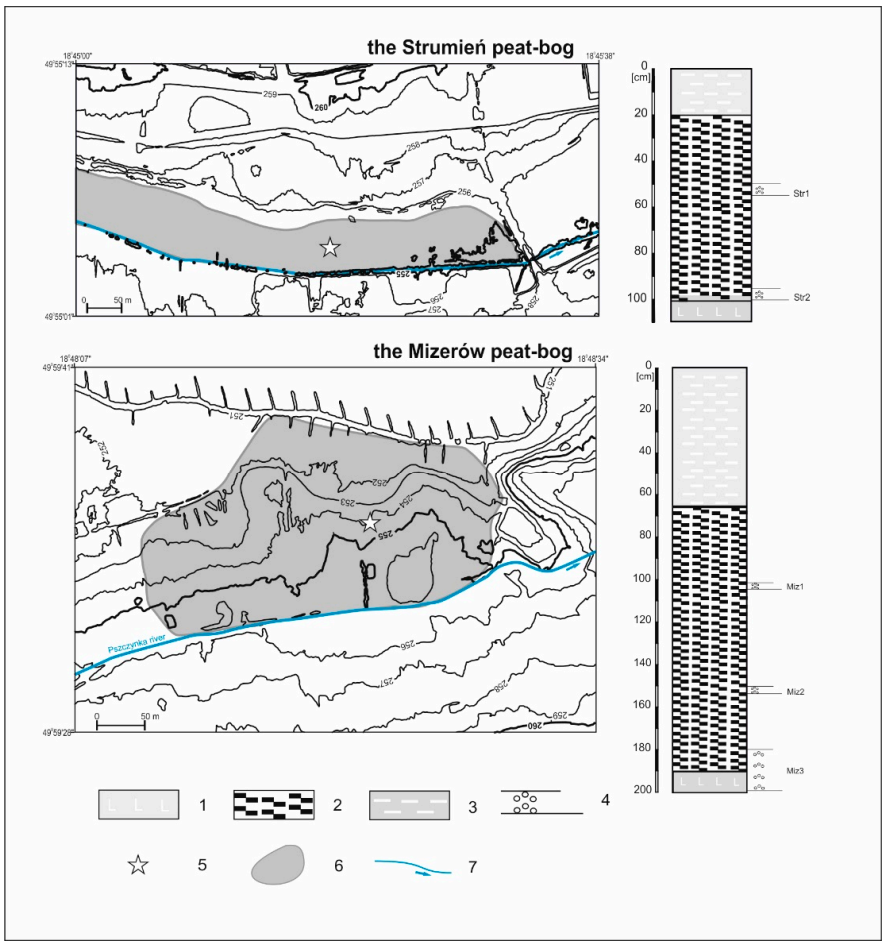

Figure 2. Lithological profiles at the Strumień and Mizerów sites. Key: 1—clay, 2—peat, 3—gyttja, 4—the investigated layers of sands, 5—sampling area, 6—peat-bog area, and 7—rivers. Str 1-2—samples of sandy layers collected from the Strumień site. Miz 1-3—samples of sandy layers collected from the Mizerów site.

2.3. Heavy Mineral Separation

High-density accessory minerals were separated from the sandy layers by using standard density-separation techniques, including: crushing, hydrofracturing, washing, Wilfley shaking table, Frantz magnetic separator and handpicking. The separation was undertaken at the Institute of Geological Sciences, Polish Academy of Sciences (Cracow, Poland).

2.4. Scanning Electron Microscope (SEM) and Electron Microprobe Analysis (EMPA)

The morphology and chemical homogeneity of the surface of selected crystals of heavy accessory minerals were investigated using a scanning FET Philips 30 electron microscope (Thermo Fisher Scientific, Waltham, MA, USA; 15 kV and 1 nA) equipped with an EDS (EDAX) detector at the University of Silesia Faculty of Earth Sciences (Sosnowiec, Poland).

Apatite mineral chemistry analyses (major and minor elements) were carried out at the Inter-Institution Laboratory of Microanalyses of Minerals and Synthetic Substances (University of Warsaw, Warsaw, Poland) using a CAMECA SX-100 electron microprobe, (CAMECA, Gennevilliers Cedex, France; 15 kV, 20 nA).

An electron microprobe was used for age determination using the Chemical Th-U-total Pb Isochron Method (CHIME) dating method of Th- and/or U-bearing minerals by Suzuki and Adachi [28,29], modified by Montel et al. [30]. For monazite mineral chemistry analyses, the operating conditions were 20 kV acceleration voltage, beam current 50 nA, beam diameter 2 μm, counting times were

200 s (2 × 100 s), and 400 s (2 × 200 s) and 600 s (2 × 300 s) for peak and background positions (in parentheses), respectively.

2.5. X-Ray Diffraction (XRD)

XRD analyses were performed on heavy minerals and powdered samples using a PANalytical X'Pert Pro MPD diffractometer (Malvern-Panalytical, Almelo, The Netherlands) powered by a PW3040/60 X-ray generator (Philips) and fitted with a 1D silicon strip detector (X'Celerator). The measurements were made using Cu Kα-radiation, with a wavelength of 0.1542 nm, an acceleration voltage of 45 kV, a current of 30 mA, and with 0.01θ step sizes between the angles of 2.5° and 65° 2θ, and a 300 s measurement time per step. The data obtained were processed using HighScore+ software and the ICSD database. All XRD analyses were performed at the University of Silesia, Faculty of Earth Sciences (in Katowice, Sosnowiec, Poland).

2.6. U-Pb Laser Ablation-Inductively Coupled Plasma Mass Spectrometry (LA-ICP-MS)

Apatite U-Pb data were acquired at the Trinity College Department of Geology (Dublin, Ireland). Twenty-eight isotopes (^{31}P, ^{35}Cl, ^{43}Ca, ^{55}Mn, ^{86}Sr, ^{89}Y, ^{139}La, ^{140}Ce, ^{141}Pr, ^{146}Nd, ^{147}Sm, ^{153}Eu, ^{157}Gd, ^{159}Tb, ^{163}Dy, ^{165}Ho, ^{166}Er, ^{169}Tm, ^{172}Yb, ^{175}Lu, ^{200}Hg, ^{204}Pb, ^{206}Pb, ^{207}Pb, ^{208}Pb, ^{232}Th, ^{238}U and mass ^{248}(^{232}Th^{16}O) were acquired using a 47 μm laser spot, a 4 Hz laser repetition rate, and a fluence of 3.31 J/cm^2. A c. 1 cm sized crystal of Madagascar apatite which has yielded a isotope dilution-thermal ionisation mass spectrometry (ID-TIMS) concordia age of 473.5 ± 0.7 Ma [31,32], was used as the primary apatite reference material in this study. McClure Mountain apatite from syenite (the rock from which the ^{40}Ar/^{39}Ar hornblende standard MMhb is derived), was used as a secondary standard. The McClure Mountain syenite has crystallization age (weighted mean ^{207}Pb/^{235}U age of 523.51 ± 2.09 Ma). The NIST 612 glass standard was used as the apatite trace-element concentration reference material, and a crushed aliquot of Durango apatite that has been characterised by solution quadrupole-ICP-MS analyses [33], was used as the apatite trace-element secondary standard.

The raw isotope data were reduced using the "Vizual Age" data reduction scheme (DRS) of Petrus and Kamber [34], within the freeware IOLITE package of Paton et al. [35]. User-defined time intervals are established for the baseline correction procedure, to calculate session-wide baseline-corrected values for each isotope. The time-resolved fractionation response of individual standard analyses is then characterised using a user-specified down-hole fractionation correction model. The data reduction scheme then fits this appropriate session-wide "model" U-Th-Pb fractionation curve to the time-resolved standard data and the unknowns. Sample-standard bracketing is applied after the correction of down-hole fractionation to account for long-term drift in isotopic or elemental ratios by normalizing all ratios to those of the U-Pb reference standards. Common Pb in the apatite standards was corrected using the ^{207}Pb-based correction method using a modified version of the VizualAge DRS that accounts for the presence of variable common Pb in the primary standard materials [36]. During the analytical session, McClure Mountain apatite (^{207}Pb/^{235}U ID-TIMS age of 523.51 ± 2.09 Ma; [37] yielded a U-Pb Tera-Wasserburg concordia lower intercept age of 517.6 ± 4.2 Ma with an MSWD = 1.4. The lower intercept was anchored using a ^{207}Pb/^{206}Pb value of value of 0.88198 derived from an apatite ID-TIMS total U-Pb isochron [37].

3. Results

3.1. Heavy Mineral Characterisation

Optical, SEM, EMPA as well as XRD observations were used to distinguish several mineral phases, including: quartz, epidote, staurolite, tourmaline (dravite and schörl), garnet, spinel, Al_2SiO_5 polymorphs (sillimanite, kyanite, andalusite), amphibole (mostly hornblende), zircon, pyroxene (e.g., richterite, diopside), perovskite, topaz, cordierite, apatite, monazite, chromite, ilmenite, illite, chlorite,

muscovite, iron oxides, rutile and siderite. These minerals are listed on Table S5. The most common and characteristic minerals were described in detail below.

3.1.1. Al_2SiO_5 Polymorphs (Kyanite, Andalusite, Sillimanite)

The investigated crystals of Al_2SiO_5 from both sites do not show any etching textures. The grains are spherical, and in most cases form grains up to 200 µm in length (Figure 3a–c). Sillimanite is present as aggregates of small and elongated crystals (aspect ratio 20:1; Figure 3c). Kyanite and andalusite were not recognized by SEM and EDS, but their presence was confirmed by XRD (Table S5). Al_2SiO_5 polymorphs were found only in the Miz 1 and Miz 2 samples.

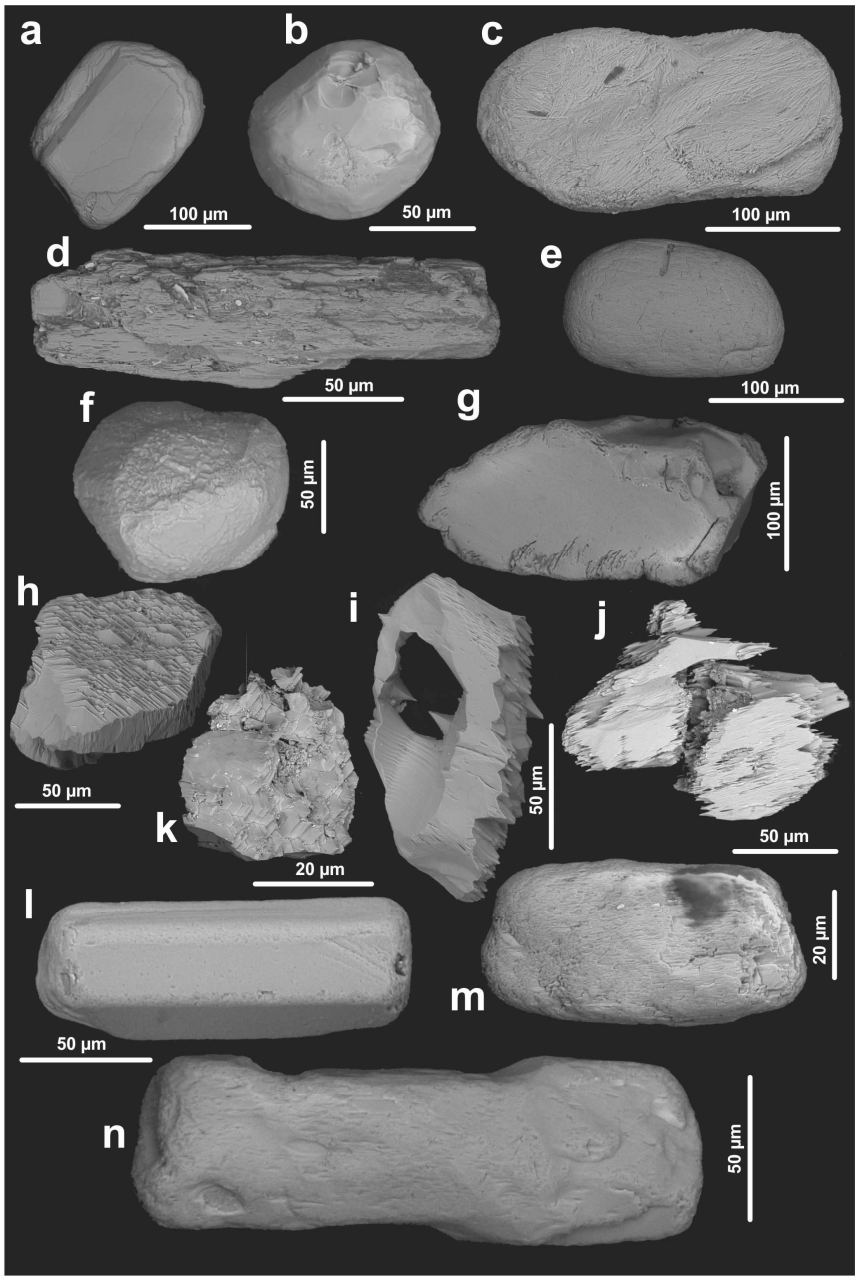

Figure 3. BSE images of selected heavy minerals from the investigated samples: (**a–c**) Al_2SiO_5 polymorphs, (**d,e**) staurolite, (**f,g**) garnet, (**h–k**) amphibole, (**l,m**) tourmaline, and (**n**) epidote.

3.1.2. Staurolite

Staurolite commonly occurs in all samples and forms spherical grains, which are up to 100 μm in diameter (Figure 3d,e). A few grains have surfaces dominated by mechanically produced features, such as breakage blocks and conchoidal fractures. EDS does not reveal any differences in the chemistry of the staurolite minerals. This mineral is characterized in all samples from the Mizerów site.

3.1.3. Garnet Group Minerals

The typical size of garnet grains is no bigger than 200 μm in diameter. Several garnet grains have smaller-scale (down to ~50 μm) surface roughness or scalloping (Figure 3f,g). Generally, the garnets do not have any faceted or conchoidal surfaces. EDS investigation show that the whole garnet population consists of spessartine, pyrope and almandine species, as well as hydrogarnets. The garnet group minerals were noted in all samples from Mizerów and the Str 1 sample.

3.1.4. Amphibole

Amphiboles were found in all studied samples. The most common type is hornblende, with a content up to ~25% in samples Miz 1 and Miz 2. The Miz 1 sample is characterised by ca. 15% actinolite. In the sample Miz 3, potassium-rich richterite is observed. In most cases, the amphibole grains are well rounded. Sometimes, the grains reveal faceted or conchoidal surfaces. A few kaersutite grains has been found in all the studied samples. Their presence was confirmed by EDS. In most cases, the kaersutite grains are up to 80 μm in size and had conchoidal edges.

3.1.5. Tourmaline

XRD investigations show that dravite dominates over schörl in all studied samples. Only in one sample (the Miz 3 sample), the schörl content reached 5 vol. %. The tourmaline grain population may be divided into two morphological types: prismatic grains with somewhat rounded edges, and rounded prisms (Figure 3l,m). The size ranges from 50 μm up to 220 μm. Tourmaline grains, especially the prismatic ones, are characterised by aspect ratios of ~3:1.

3.1.6. Epidote Group Minerals

The grain habit of epidote in ythe investigated samples is prismatic, and sometimes exhibit slender, prismatic forms (Figure 3n). Only in a few cases was the epidote well-rounded. The grains vary in size from 80 μm to 150 μm and were found in the Miz 2 and Miz 3 sample.

3.1.7. Apatite

Two different morphological types of apatites were found only in the Strumień peat-bog. All grains were handpicked from the heavy mineral concentrate. The first apatite type is composed of elongated crystals or its fragments. Locally, these apatite grains show strong abrasion, but in most cases the grains reveal sharp edges, and well-defined crystal faces (Figure 4A). Their size varies from c. 10 μm to 80 μm. The second apatite type is characterised by spherical grains. They are up to 50–80 μm in diameter (Figure 4C). Both types were used for REE and U-Pb age determinations. The first type of apatite is characterized by the REE patterns typical of igneous apatites e.g., [38–40], with LREE predominating over the HREE (Table S6; Figure 4B). The first sample from the Strumień site is characterized by strong REE fractionation (avg. $(Ce/Yb)_N$ = 21.57), positive Eu anomalies (avg. Eu/Eu* = 1.08) and slightly negative Ce anomalies (avg. Ce/Ce* = 0.98). Only the first type gave a meaningful result from U-Pb LA-ICP-MS dating, yielding an anchored lower intercept age of 116 ± 12 Ma (MSWD = 3.1; Table S7; Figure 4A). Dating of the second type of apatites in the samples failed to give meaningful data (Table S7, Figure 4C). However, the REE fractionation in these apatites is characterised by strong fractionation (avg. $(Ce/Yb)_N$ = 56.47), and slightly negative Eu anomalies (avg. Eu/Eu* = 0.81) and positive Ce anomalies (avg. Ce/Ce* = 1.01; Table S6, Figure 4D).

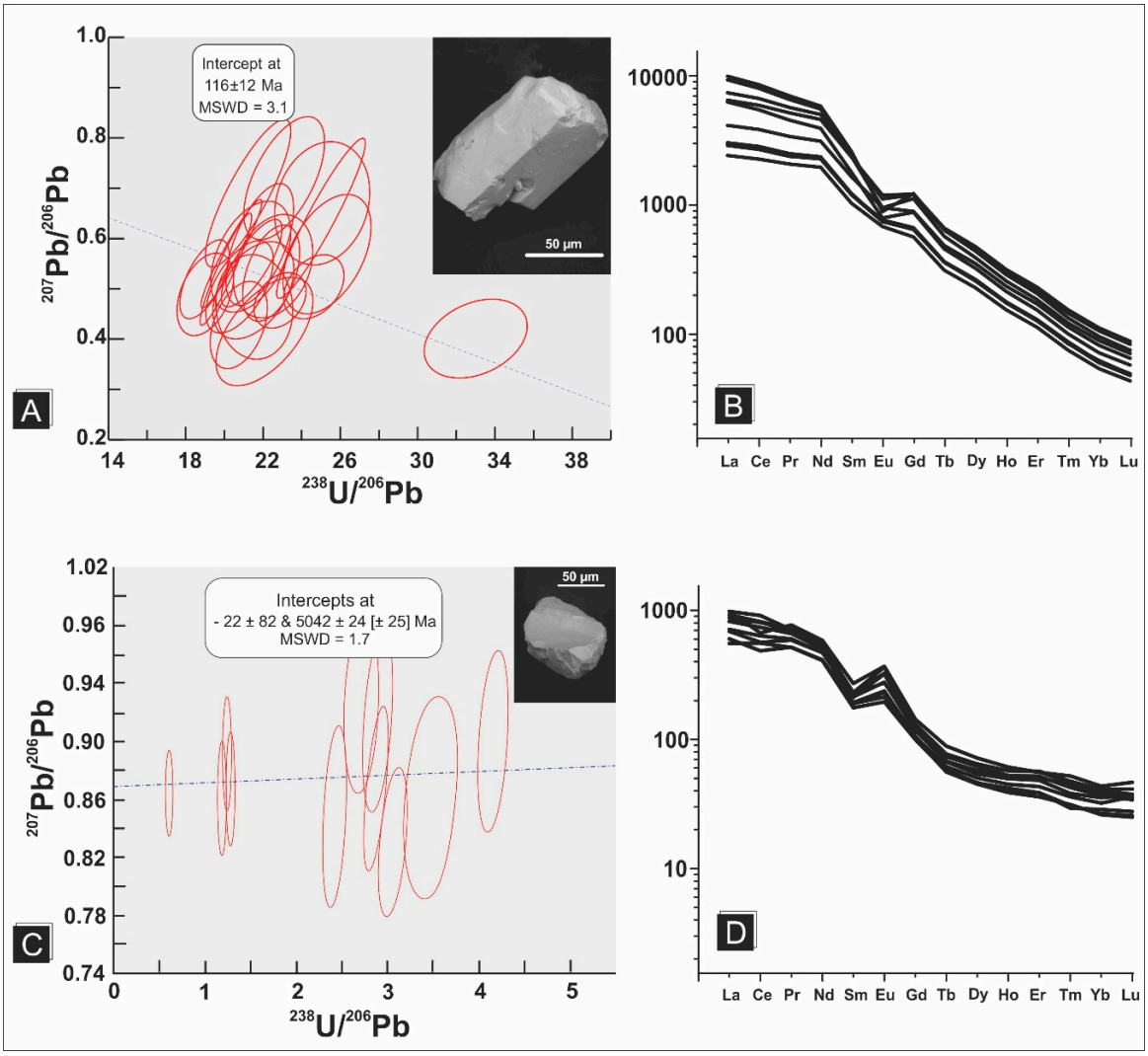

Figure 4. (**A**) Tera-Wasserburg concordia plot for LA-ICPMS U-Pb apatite analyses (~120 Ma) and (**B**) chondrite (C1)-normalized REE diagram for the first apatite type. (**C**) The second apatite morphology did not yield a meaningful U-Pb age due to high common Pb contents. (**D**) Chondrite (C1)-normalized REE diagram for the second apatite type.

3.1.8. Monazite

The monazite grains, which were classified as Ce-rich monazite, reaching c. 80–90 µm in size, were hand-picked from the Mizerów sample. Five grains of (Ce)-monazite were used for morphological and chemical characterisation. The investigated grains show slightly weak internal zoning (Table S8). The CHIME ages [28–30] were calculated based on their chemical composition. All ages are Variscan. The weighted mean age is 332 ± 3 Ma (MSWD = 5.64; Figure 5). Moreover, four older (ca. 466 Ma, ca. 426 Ma, ca. 386 Ma, and ca. 358 Ma), and one younger (ca. 337 Ma) ages were also obtained (Figure 5).

3.1.9. Zircon

In the zircon population, numerous different crystal morphologies were identified (Figure 6a,b). Up to 20% of all inspected zircon crystals reveal prismatic shapes and habit (Figure 6c–e). The rest of the grains range from slightly rounded (c.a. 15%), prismatic and subhedral shapes to sub-rounded types (c.a. 10%). Sporadically, spherical forms were also noted. Zircon crystals are characteristic for all samples from the Mizerów site.

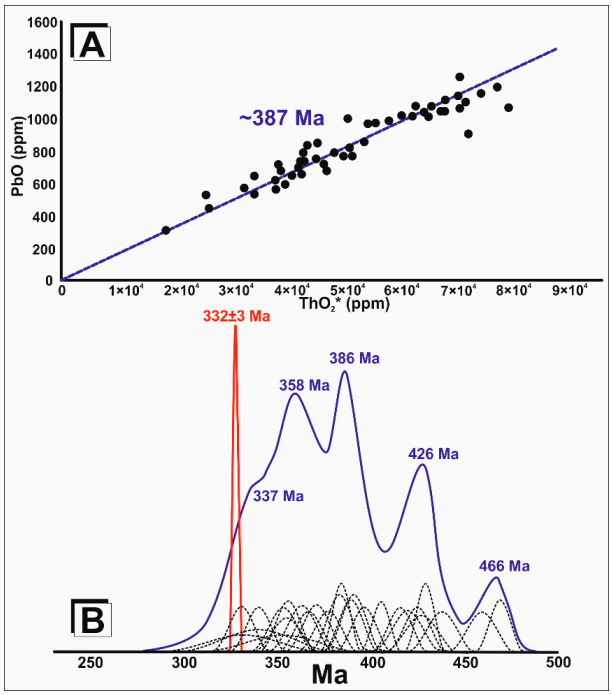

Figure 5. (**A**) Plot of PbO vs. ThO_2* for a monazite grain from the Mizerów sample according to the CHIME procedure. ThO_2*—the real Th content was calculated as a oxide, including correction for U. (**B**) Histogram based on 39 EMP spot analyses performed on monazite using Montel's method [30]. Three major age populations are indicated at ~430, ~360, and ~310 Ma. The mean weighted age is 332 ± 3 Ma (MSWD = 5.64).

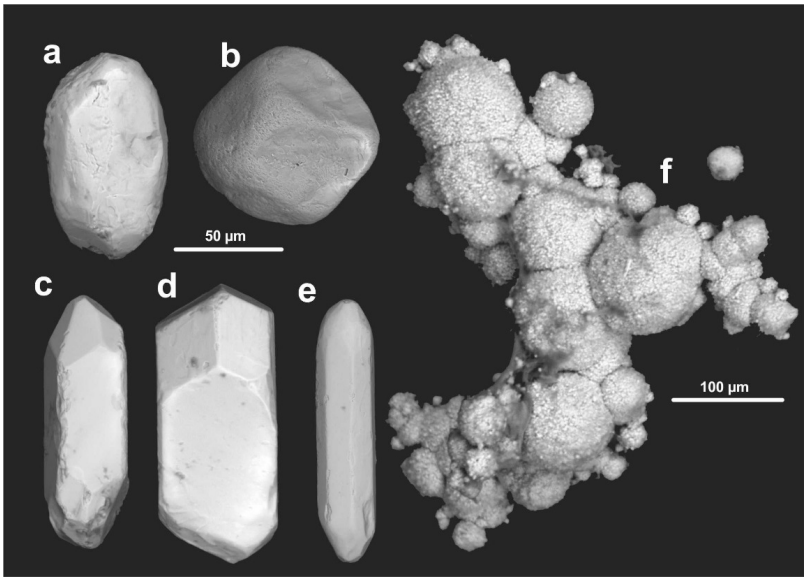

Figure 6. BSE image of selected zircon and pyrite grains. (**a**,**b**) Well-rounded zircon grains. (**c**–**e**) An example of prismatic, well developed zircons. (**f**) An example of framboidal pyrite aggregates associated with the studied sediments.

3.1.10. Authigenic Heavy Minerals

The authigenic heavy mineral suite is limited to a few framboidal pyrite aggregates, which were found on the margin with the peat (Figure 6f). The pyrite, both framboids and cube-like-octahedral forms, are the most common heavy mineral in the surrounding peat units.

4. Discussion

4.1. Transport Type

During the Quaternary, the most significant environmental and geographic changes in the regional drainage basins took place with the development of the contemporary fluvial network of the upper Vistula River Valley [21]. Based on pollen analysis of the Strumień site peat, the subatlantic period has been recognized. However, data obtained by Pazdur [41] in the Pszczynka valley indicate the accumulation of peat in this area for the entire duration of the Holocene [42]. The presence of the locally accumulated layers of sand in the studied profiles is likely related to a floodplain environment dominated by wetlands and riverside marshes. These environments are suitable for peat bogs and phytogenic deposit formation [43], with the layers of sandy material in the peat indicating periods of flooding. Isolated and numerous ephemeral floods, as well as periods of sustained rainfall were characteristic in this area during Holocene and caused significant changes in the river valleys [44]. There were no significant climate fluctuations in both the subboreal and subatlantic periods [45]. During these intervals, palynological data show an increase in the presence of vegetation as a result of human activity. The pollen analysis for the Strumień site showed dense but treeless vegetation, which may also inhibit aeolian deposition. Horizons with high concentrations of heavy minerals accumulated mostly through alluvial transport but aeolian transport cannot be excluded as a different process leading to the formation of heavy mineral-rich sands. Alluvial reworking of aeolian deposits that concentrate heavy minerals can produce rounding of grains, such as that observed in most samples (Figures 3 and 6). In addition, the lack of muscovite (Sample Miz 1, Miz 3, and Str 2), and chlorite (Sample Miz 1 and Miz 2), defined by Chlebowski and Lindner [46] as minerals susceptible to deflation and aeolian transport, is an indication that aeolian processes are not predominant. In the literature, an increase in tourmaline content is associated with aeolian processes [8]. However, in the results obtained only in the sample Str 1 (depth 0.50–0.55 m), tourmaline content reaches a value above 20%. There are key differences between the studied heavy mineral-rich sediments from both the Strumień and Mizerów sites (Figures 3 and 6). Actinolite, garnet, ilmenite, andalusite, chlorite and zircon dominate in the Mizerów site, while tourmaline, hornblende, rutile, muscovite and magnetite are characteristic for the Strumień site. Generally, at both peat-bogs studied, the characteristic features of the heavy mineral suite can be used for catchment area reconstruction. This can be done in case of sediments, where less resistant primary components (e.g., feldspar, olivine), have been eliminated by weathering processes.

Staurolite and Al_2SiO_5 polymorphs, when present, appear to be the most suitable for assessing the intensity of weathering in the peat sediments. This, in turn, may allow for an assessment of the other minerals. For instance, strongly weathered staurolite in a sample likely indicates that minerals that are more susceptible to weathering, such as topaz or corundum, were eliminated. The presence of staurolite, often associated with andalusite and kyanite, in regionally metamorphosed rocks, and provides information on sand provenance. This situation is characteristic for the Mizerów site. Moreover, staurolite, kyanite, andalusite, zircon, tourmaline and hornblende, especially from the Strumień site, appear to have been resistant to acidic leaching.

The distribution of zircon is variable in the studied sites. The presence of rounded and subrounded zircon may indicate a relatively strong reworking, with most grains probably coming from igneous or metamorphic rocks. Provenance areas include from the Bohemian Massif or the Tatra Massif. No zircon crystals were found in the Strumień site.

The highest mean abundance of rutile was found in the Strumień site (up to 22 vol. %), while the Mizerów site sample is characterised by lower rutile content (up to 5 vol. %; Table S5). The rutile population is represented by grains with differences in size and shape. Some of the grains show typical bladed or prismatic characters, with well-developed cleavage traces or less common leaching edges. The presence of rounded rutile indicates reworked sediments, most probably coming from metamorphic source rocks.

The epidote population, in almost all investigated grains, lacks corrosion textures, with grains retaining typical bladed or prismatic habits, with well-developed cleavage planes. In some cases, early stages of epidote corrosion are manifested by oriented pits, but as dissolution proceeds, epidote develops large-scale 'hacksaw' terminations. This situation has been described in many sediments [47–49]. Epidote can form as a rock-forming mineral, typically as products of regional metamorphism, and in some felsic igneous rocks as well as in hydrothermally altered rocks. Epidote group minerals are common products in calcareous sedimentary rocks in contact metamorphic aureoles. They can also be found in pegmatites and granites as primary magmatic phases, as well as secondary phases (e.g., plagioclase-saussuritization) e.g., [50,51].

Phosphates are represented by (Ce)-monazite and fluorapatite. Both species are common accessory minerals in igneous and metamorphic rocks of different chemistry and provenance. Phosphates, especially monazite and apatite, are suitable for geochronology. The monazite population seems to have a magmatic origin as it exhibits internal magmatic zoning. The main monazite CHIME age (Figure 5), may be interpreted as the Variscan magmatic event, which is widely observable in numerous nearby plutons [52–54], and references therein. The obtained U-Pb apatite LA-ICP-MS age, chemical homogeneity of the grains and REE profiles implies a magmatic source (Figure 4A,B). The origin of the second apatite population is less clear (Figure 4C,D). The REE patterns are more characteristic of metamorphic or hydrothermal apatite cf [55,56].

4.2. Heavy Mineral Provenance Area Characterization

Two different source rock areas, the Tatra Mountains and the Sudety Mountains, are indicated for both investigated peat-bog sites. The Tatra Mountains are an example of a complex crystalline massif, composed of polygenic granitoid intrusions which are partly covered by its metamorphic envelope in the western region [52] and references therein. The metamorphic cover is composed of gneisses, schists, amphibolites, and locally also eclogites [53,57] and references therein. This massif, uplifted during Alpine orogenesis [58], could be the source of detrital minerals in this study, which are eroded and transported away from the Carpathians by rivers. The Vistula and the Danube rivers are the largest rivers that transport material from the Tatra Mountains to the north and the Carpathians to the south of the sampling sites respectively.

The detrital mineral suite, produced by weathering and erosion of rocks from the Tatra Mountains, is dominated by magmatic components such as zircon, tourmaline, apatite. However, because the metamorphic envelope is mostly located on southern part of the crystalline core in Slovakia, all detrital metamorphic grains sourced from the Tatras (kyanite, sillimanite, garnet, staurolite, amphibole (mostly hornblende), would likely be transported to the south.

The Bohemian Massif is one of the largest continuously outcropping fragments of the extensive Variscan basement that crops out beneath the Variscan platform and younger sediments. The Bohemian Massif is a complex geological area with numerous granitoid intrusion types and metamorphic units. Due to its size and tectonic character, several regions differ in lithology and age and can be readily distinguished. They are as follows: the Moldanubian, Teplá-Barrandian, Saxo-Thuringian (subdivided by the younger Elbe Fault Zone into the Krušné Hory mountain zone and the Lugicum-West Sudetic Zone) and Moravo–Silesian units e.g., [59]. The Moravo-Silesian Unit is the nearest unit and is located to the west from both investigated peat sites. The eastern region is the Bardzkie Mountains, which are a part of the Kłodzko-Złotostocki Massif (the Central Sudetes). The whole massif is a potential source for a diverse suite of heavy minerals, but in the most eastern part, metamorphic assemblages dominate.

The third possible supply area for the studied material is the teschenite-picrite association (TPA) rocks. Generally, these rocks are exposed between the Bohemian Massif (the Sudetes) and the Tatra Massif. This early Cretaceous alkaline volcanic region, of which the TPA of volcanic rocks are associated, is unique to the western part of the Outer Western Carpathians. This magmatic province is 15–25 km wide and extends in a NE direction for over 100 km from Hranice in Moravia, the Czech Republic, to Cieszyn and Bielsko-Biała in Poland (the Silesian Basin; Figure 1). The TPA contains a wide range of

intrusive rocks, which belong to two main groups of alkaline (teschenite, picrite, syenite, lamprophyre) and sub-alkaline (typically dolerite) igneous rocks. The most common heavy minerals related to the TPA are: diopside, clinopyroxene, amphibole (kaersutite), mica (annite-siderophyllite), chlorite, haematite, apatite and titanite. The timing of volcanic activity of the TPA in the Silesian Basin took place from 128 to 103 Ma, and most likely peaked between 128–120 Ma [60–63].

4.3. Development of Relief and River System in Neogene and Pleistocene

Heavy minerals are one of the best indicators of the origin of terrigenous detrital material, and allow for the determination of provenance areas for sediments whose primary components, especially those less resistant to weathering, have been eliminated by weathering processes. In the studied area, the most crucial factor for determining the mineral transport directions was the regional river valley evolution. The transport and accumulation of detrital material occurred in several phases within the Moravian Gate and its surrounding areas. In the initial phase of river formation in the Pleistocene, the main direction of fluvial outflow was dominated by a river (pre-Odra) [64] on the Fore-Sudetic Block, which was flowing from the present Silesian Uplands and the Eastern Sudetes. The river flowed broadly north-east, meandering over the Fore-Sudetic block and sporadically overflowing its flood plain.

In Pliocene and Early Pleistocene, the hydrographic network was modified. The newly created Odra Valley became the drainage area for the Carpathian basin. Numerous modifications in the drainage basin caused by glacial transgressions lead to changes in the flow directions of all the Carpathian rivers. The modern northern Vistula tributaries (Pszczynka, Gostynka) also experienced a modification of its drainage network (Figure 7). The studied area of the Oświęcim Basin is located within the region of the South Polish Glaciations (Elsterian), where two episodes of the Saalian I stage [64] are fingerprinted. The climate changes (mostly cooling) during the Dryas stage was responsible for the river debris increasing in the Carpathian area [64].

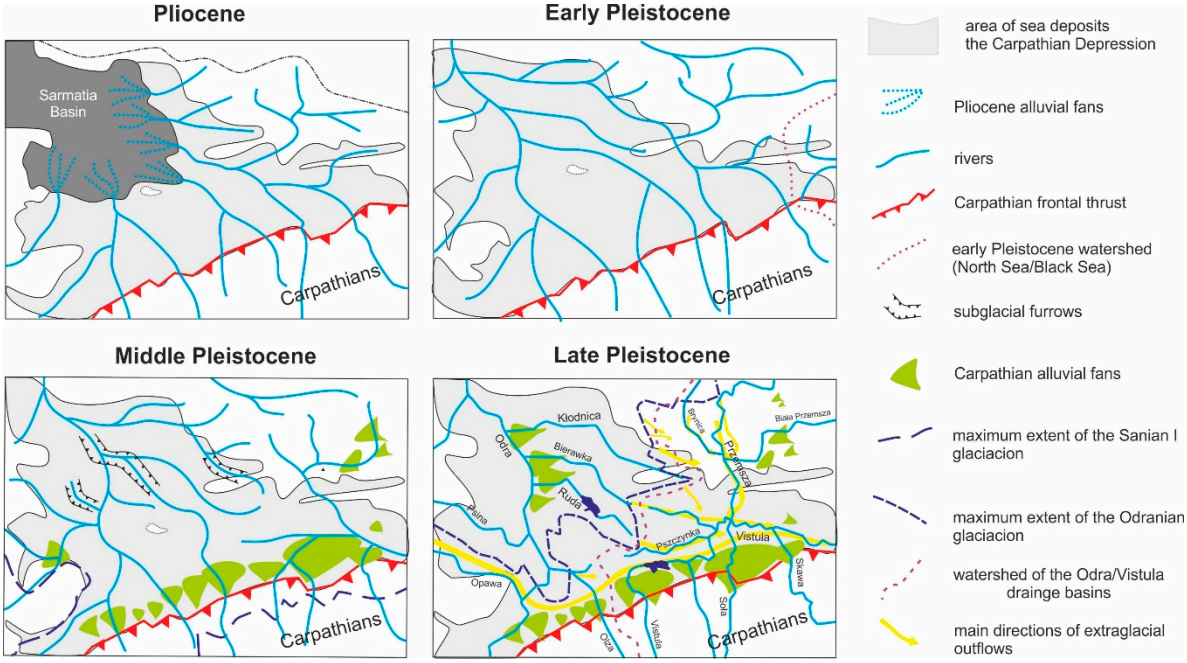

Figure 7. Simplified sketch showing the evolution of the river network patterns in the Racibórz-Oświęcim Basin during the late Neogene and Pleistocene. Modified after [23].

During the next stage (Early Pleistocene?) which was characterized by intense landscape weathering, the regional river system was formed, and has continued in this configuration with minor

changes up to the present day. The main river channel (pre-Odra) in the western part of the study area shifted north, probably beyond the line of the present-day Odra channel, while a system of local river valleys flowing from the Sudetes developed on the Fore-Sudetic block, and rivers drained the Sudetes Mountains [63,65–68]. River network modifications of the whole Vistula River Valley occurred at the Vistulian/Holocene boundary. Subsequently annual flood-thaw cycles were replaced by more common rain floods. At this time, braided rivers changed into meandering fluvial systems [64,69]. Starkel [70–73] indicated that climate changes in Holocene supported cyclic inundation of the Upper Vistula River Valley, which could be responsible for redeposition and/or mixing of all previously deposited sediments. The present-day Vistula River represents mostly a braided river, overcharged with sediments [69], mainly as a result of human activity in the catchment areas.

5. Conclusions

This paper presents a detailed characterisation of heavy minerals from peats in the Carpathian Foredeep in Poland.

(1) The studied heavy mineral suite reveals up to three different source areas, which were confirmed by mineral composition and age.
(2) These different source areas are: (a) the Tatra Massif, (b) the Bohemian Massif, and (c) the Silesian Basin area. However, some parts of the mineral assemblages may point to the South Polish Glaciations (Elsterian) sediments as the source. Originally, this material could have been deposited in the Oświęcim Basin by glaciers.
(3) The studied heavy mineral suite as well as sedimentology indicates an alluvial origin related to both the Odra (praOdra) and the Vistula valley development. Any aeolian component for the provenance of the material is insignificant.
(4) Numerous mineral grains reveal characteristic dissolution features caused by long-term stagnation in a water-rich environment.

Supplementary Materials: The following are available online at http://www.mdpi.com/2075-163X/10/1/9/s1, Table S1: Simplified lithological profile including peat classifications from the Strumień site [25,27], Table S2: Plant macro-remains identified from the Strumień site, Table S3: Simplified lithological profile including peat classifications from the Mizerów site [25,27], Table S4: Plant macro-remains identified from the Mizerów site, Table S5: Mineral composition based on X-ray diffraction of investigated heavy fraction from the sandy layers from the Strumień and Mizerów sites, Table S6: Representative LA-ICPMS apatite REE analyses from this study, Table S7: Representative LA-ICPMS U-Pb apatite data for samples from this study, Table S8: Representative EMPA monazite data and their chemical formulae based on $4O^{2-}$.

Author Contributions: K.S., S.S., and A.S. wrote the paper. S.S. and K.S. collected the studied material. D.C. and T.K. obtained U-Pb and powder X-ray diffraction data, respectively. K.S. obtained EMPA and calculated the CHIME age. S.S. and A.S. recognized the flora. All authors have read and agreed to the published version of the manuscript.

Funding: This work was financially supported by the Institute of Earth Sciences at the Faculty of Natural Sciences, University of Silesia in Katowice, Poland. DC acknowledges support from research grant 13/RC/2092 from Science Foundation Ireland which is co-funded under the European Regional Development Fund and by PIPCO RSG and its member companies.

Acknowledgments: The authors benefitted greatly from discussions with Aleksandra Gawęda. Ashley P. Gumsley is thanked for language editing and comments on the script. Lidia Jeżak and Piotr Dzierżanowski are thanked for their help during the microprobe analyses.

Conflicts of Interest: The authors declare no conflict of interest.

References

1. Kalińska-Nartiša, E.; Stivrins, N.; Grudzinska, I. Quartz grains reveal sedimentary palaeoenvironment and past storm events: A case study from eastern Baltic. *Estuar. Coast. Shelf Sci.* **2018**, *200*, 359–370. [CrossRef]
2. Racinowski, R. Niektóre problemy interpretacji wyników analiz minerałów ciężkich w badaniach osadów czwartorzędowych. *Przegląd Geol.* **2010**, *48*, 354–359. (In Polish)

3. Bateman, R.M.; Catt, J.A. Provenance and palaeoenvironmental interpretation of superficial deposits, with particular reference to post-depositional modification of heavy mineral assemblages. *Dev. Sedimentol.* **2007**, *58*, 151–188. [CrossRef]
4. Yang, D.; Yu, G.; Xie, Y.; Zhan, D.; Li, Z. Sedimentary records of large Holocene floods from the middle reaches of the Yellow River, China. *Geomorphology* **2000**, *33*, 73–88. [CrossRef]
5. Hagedorn, E.-M.; Boenigk, W. The Pliocene and Quaternary sedimentary and fluvial history in the Upper Rhine Graben based on heavy mineral analyses. *Neth. J. Geosci. Geol. En Mijnb.* **2007**, *87*, 21–32. [CrossRef]
6. Weckwerth, P.; Chabowski, M. Heavy minerals as a tool to reconstruct river activity during the Weichselian glaciation (Toruń Basin, Poland). *Geologos* **2013**, *19*, 25–46. [CrossRef]
7. Wachecka-Kotkowska, L.; Ludwikowska-Kędzia, M. Heavy–mineral assemblages from fluvial Pleniglacial deposits of the Piotrków Plateau and the Holy Cross Mountains—A comparative study. *Geologos* **2013**, *19*, 131–146. [CrossRef]
8. Marcinkowski, B.; Mycielska-Dowigałło, E. Heavy-mineral analysis in Polish investigations of Quaternary deposits: A review. *Geologos* **2013**, *19*, 5–23. [CrossRef]
9. Morton, A.C.; Smale, D. The effects of transport and weathering on heavy minerals from the Cascade River, New Zealand. *Sediment. Geol.* **1990**, *68*, 117–123. [CrossRef]
10. Woronko, B.; Rychel, J.; Karasiewicz, M.T.; Ber, A.; Krzywicki, T.; Marks, L.; Pochocka-Szwarc, K. Heavy and light minerals as a tool for reconstruction of depositional environments: An example from the Jałówka site (northern Podlasie region, NE Poland). *Geologos* **2013**, *19*, 47–66. [CrossRef]
11. Dill, H.G. Grain morphology of heavy minerals from marine and continental placer deposits, with special reference to Fe–Ti oxides. *Sediment. Geol.* **2007**, *198*, 1–27. [CrossRef]
12. Komar, P.D. The entrainment, transport and sorting of heavy minerals by waves and currents. *Dev. Sedimentol.* **2017**, *58*, 3–48. [CrossRef]
13. Krzyszkowski, D. Stratygrafa, petrografa i paleogeografa glin lodowcowych [Till stratigraphy, petrography and palaeogeography along the northwestern coastal region of Poland]. *Biul. Państwowego Inst. Geol.* **2010**, *438*, 51–91. (In Polish)
14. Thamó-Bozsó, E.; Magyari, Á.; Nagy, A.; Unger, Z.; Kercsmár, Z. Osl Dates and heavy mineral analysis of upper Quaternary sediments from the Valleys of The Ér and Berettyó Rivers. *Geochronometria* **2007**, *28*, 17–23. [CrossRef]
15. Żytko, K.; Zając, R.; Gucik, S.; Ryłko, W.; Oszczypko, N.; Garlicka, I.; Nemčok, J.; Eliáš, M.; Menčik, E.; Stránik, Z. *Map of the Tectonic Elements of the Western Outer Carpathians and Their Foreland*; Poprawa, D., Nemčok, J., Eds.; Geological Atlas of the Western Outer Carpathians and their Foreland; Państwowy Instytut Geologiczny, Warszawa/GUDŠ Bratislava/Uug Praha: Warszawa, Poland, 1989.
16. Włodyka, R. *The Evolution of Mineral Composition of the Cieszyn Magma Province Rocks*; Wydawnictwo Uniwersytetu Śląskiego: Katowice, Poland, 2010; pp. 1–232. (In Polish)
17. Kondracki, J. *Geografa Polski. Mezoregiony Fzyczno-Geografczne*; Państwowe Wydawnictwo Naukowe: Warsaw, Poland, 1995; pp. 35–37. (In Polish)
18. Marks, L.; Ber, A.; Gogołek, W.; Piotrowska, K. *Geological Map of Poland 1:500,000, with Explanatory Text*; Państwowy Instytut Geologiczny: Warszawa, Poland, 2006.
19. Marks, L. Quaternary glaciations in Poland. *Dev. Quat. Sci.* **2011**, *15*, 299–303. [CrossRef]
20. Niedziałkowska, E.; Gillot, E.; Pazdur, M.F.; Szczepanek, K. The Upper Vistula Valley near Drogomyśl in the Late Vistulian and Holocene. *Folia Quat.* **1985**, *56*, 101–132.
21. Starkel, L. *Historia Doliny Wisły od Ostatniego Zlodowacenia do Dziś*; IGiPZ PAN: Warsaw, Poland, 2001; pp. 47–53. (In Polish)
22. Niedziałkowska, E.; Szczepanek, K. Utwory pyłowe vistuliańskiego stożka Wisły w Kotlinie Oświęcimskiej. *Studia Geomorphol. Carpato-Balc.* **1994**, *27*, 29–44. (In Polish)
23. Lewandowski, J. Plejstocen glacjalny Kotliny Raciborsko–Oświęcimskiej i obszarów sąsiednich. In *X Konferencja Stratygraficzna Plejstocenu Polski; Rudy, Poland, 01–05.09.2003*; Hasing, J., Lewandowski, J., Eds.; W&W: Sosnowiec, Poland, 2003; pp. 25–26. (In Polish)
24. Lewandowski, J. Jurajska Oaza Śródlądowa w świetle badań ostatniego półwiecza. *Przegląd Geol.* **2011**, *59*, 732–738. (In Polish)
25. Tołpa, S.; Jasnowski, M.; Pałczyński, A. System der genetischen Klassifizierung der Torfe Mitteleuropas. *Zesz. Probl. Postępów Nauk Rol.* **1967**, *76*, 9–99.

26. Tobolski, K. *Przewodnik do Oznaczania Torfów i Osadów Jeziornych*; Vademecum Geobotanicum 2; Wydawnictwo Naukowe PWN: Warsaw, Poland, 2000; p. 508. (In Polish)
27. Rydin, H.; Jeglum, J.K. *The Biology of Peatlands. Biology of Habitats*, 2nd ed.; Oxford University Press: Oxford, UK, 2013; p. 93.
28. Suzuki, K.; Adachi, M. Precambrian provenance and Silurian metamorphism of the Tshubansowa paragneiss in the South Kitakami terrane, northeast Japan revealed by chemical Th-U-total Pb isochrone ages from monazite, zircon, and xenotime. *Geochem. J.* **1991**, *25*, 357–376. [CrossRef]
29. Suzuki, K.; Adachi, M. The chemical Th-U-total P isochron ages of zircon and monazite from the Gray Granite of Hida terrane, Japan. *J. Earth Planet. Sci. Nagoya Univ.* **1994**, *38*, 11–37.
30. Montel, J.M.; Foret, S.; Veschambre, M.; Nicollet, C.; Provasta, A. Electron microprobe dating of monazites. *Chem. Geol.* **1996**, *131*, 37–53. [CrossRef]
31. Cochrane, R.; Spikings, R.A.; Chew, D.; Wotzlaw, J.F.; Chiaradia, M.; Tyrrell, S.; Schaltegger, U.; Van der Lelij, R. High temperature (>350 °C) thermochronology and mechanisms of Pb loss in apatite. *Geochim. Et Cosmochim. Acta* **2014**, *127*, 39–56. [CrossRef]
32. Thomson, S.N.; Gehrels, G.E.; Ruiz, J.; Buchwaldt, R. Routine low-damage apatite U–Pb dating using laser ablation-multicollector-ICPMS. *Geochem. Geophys. Geosystems* **2012**, *13*, Q0AA21. [CrossRef]
33. Chew, D.M.; Babechuk, M.G.; Cogné, N.; Mark, C.; O'Sullivan, G.J.; Henrichs, I.A.; Doepke, D.; McKenna, C. (LA,Q)-ICPMS trace-element analyses of Durango and McClure Mountain apatite and implications for making natural LA-ICPMS mineral standards. *Chem. Geol.* **2016**, *435*, 35–48. [CrossRef]
34. Petrus, J.A.; Kamber, B.S. VizualAge: A Novel Approach to Laser Ablation ICP-MS U-Pb Geochronology Data Reduction. *Geostand. Geoanalytical Res.* **2012**, *36*, 247–270. [CrossRef]
35. Paton, C.; Helistrom, J.; Paul, B.; Woodhead, J.; Herqt, J. Iolite: Freeware for the visualisation and processing of mass spectrometric data. *J. Anal. At. Spectrom.* **2011**, *26*, 2508–2518. [CrossRef]
36. Chew, D.M.; Petrus, J.A.; Kamber, B.S. U-Pb LA-ICPMS dating using accessory mineral standards with variable common Pb. *Chem. Geol.* **2014**, *363*, 185–199. [CrossRef]
37. Schoene, B.; Bowring, S.A. U-Pb systematics of the McClure Mountain syenite: Thermochronological constraints on the age of the Ar-40/Ar-39 standard MMhb. *Contrib. Mineral. Petrol.* **2006**, *151*, 615–630. [CrossRef]
38. Gawęda, A.; Szopa, K.; Chew, D. LA-ICP-MS U-Pb dating and REE patterns of apatite from the Tatra Mountains, Poland as a monitor of the regional tectonomagmatic activity. *Geochronometria* **2014**, *4*, 306–314. [CrossRef]
39. Szopa, K.; Gawęda, A.; Müller, A.; Sikorska, M. The petrogenesis of granitoid rocks unusually rich in apatite in the Western Tatra Mts. (S-Poland, Western Carpathians). *Mineral. Petrol.* **2013**, *107*, 609–627. [CrossRef]
40. Szopa, K.; Brachaniec, T.; Krzykawski, T. Preliminary EMPA and XRD investigation on detrital minerals from the Štramberk Limestone in the Czech Republic. *Neues Jahrb. Fur Geol. Und Palaontol. Abh.* **2015**, *276*, 201–212. [CrossRef]
41. Pazdur, A. *Sprawozdanie z Wykonania Oznaczeń 14C w Laboratorium 14C Instytutu Fizyki Politechniki Śląskiej w Gliwicach*; Narodowe Archiwum Geologiczne PIG-PIB: Warszawa, Poland, 1998. (In Polish)
42. Wójcik, A.; Nescieruk, P. *Objaśnienia do Szczegółowej Mapy Geologicznej Polski 1:50,000*; Arkusz Pszczyna (992): Warszawa, Poland, 2013. (In Polish)
43. Gradziński, R.; Kostecka, A.; Radomski, A.; Unrug, R. *Zarys Sedymentologii*, 1st ed.; Wydawnictwo Geologiczne: Warszawa, Poland, 1986; pp. 398–407. (In Polish)
44. Ralska-Jasiewiczowa, M.; Starkel, L. Record of the hydrological changes during the Holocene in the lake, mire and fluvial deposits of Poland. *Folia Quat.* **1988**, *57*, 91–127.
45. Lindner, L.; Lamparski, Z.; Madeyska, T.; Marks, L.; Różycki, S.T. *Czwartorzęd*; Lindner, L., Ed.; Wydawnictwa PAE: Warszawa, Poland, 1992; pp. 615–618. (In Polish)
46. Chlebowski, L.; Lindner, L. Aspekty mineralogiczne w metodyce badań lessów na przykładzie lessów polskich i ukraińskich. [Mineralogical issues in the methodology of loess analysis with examples from loesses of Poland and Ukraine]. In *Geneza, Litologoa i Stratygrafia Utworów Czwartorzędowych [Genesis, Lithology and Stratygraphy of Quarternary Deposits]*; Kostrzewski, A., Ed.; Adam Mickiewicz University: Poznań, Poland, 2004; pp. 17–36.

47. Turner, G.; Morton, A.C. The effects of burial diagenesis on detrital heavy mineral grain surface textures. In *Developments in Sedimentology 58*; Mange, M.A., Wright, D.T., Eds.; Elsevier: Amsterdam, The Netherlands, 2007; pp. 393–412. [CrossRef]
48. Morton, A.C. Surface textures of heavy mineral grains from the Palaeocene of the central North Sea. *Scott. J. Geol.* **1979**, *15*, 293–300. [CrossRef]
49. Morton, A.C. Stability of detrital heavy minerals in Tertiary sandstones of the North Sea Basin. *Clay Miner.* **1984**, *19*, 287–308. [CrossRef]
50. Janeczek, J.; Sachanbinsk, M. Babingtonite, Y-Al-rich titanite, and zoned epidote from the Strzegom pegmatites, Poland. *Eur. J. Mineral.* **1992**, *4*, 307–320. [CrossRef]
51. Morad, S.; El-Ghali, M.A.K.; Caja, M.A.; Sirat, M.; Al-Ramadan, K.; Mansurbeg, H. Hydrothermal alteration of plagioclase in granitic rocks from Proterozoic basement of SE Sweden. *Geol. J.* **2010**, *45*, 105–116. [CrossRef]
52. Gawęda, A.; Burda, J.; Klötzli, U.; Golonka, J.; Chew, D.; Szopa, K. Episodic construction of the Tatra granitoid intrusion (Central Western Carpathians, Poland/Slovakia): Consequences for the geodynamics of Variscan collision and Rheic Ocean closure. *Int. J. Earth Sci. (Geol. Rundsch.)* **2016**, *105*, 1153–1174. [CrossRef]
53. Gawęda, A.; Burda, J.; Golonka, J.; Klötzli, U.; Szopa, K.; Wiedenbeck, M. The evolution of Eastern Tornquist-Paleoasian Ocean and subsequent continental collisions: A case study from the Western Tatra Mountains, Central Western Carpathians (Poland). *Gondwana Res.* **2017**, *48*, 134–152. [CrossRef]
54. Kryza, R.; Pin, C.; Oberc-Dziedzic, T.; Crowley, Q.G.; Larionov, A. Deciphering the geochronology of a large granitoid pluton (Karkonosze Granite, SW Poland): An assessment of U–Pb zircon SIMS and Rb–Sr whole-rock dates relative to U–Pb zircon CA-ID-TIMS. *Int. Geol. Rev.* **2014**, *56*, 756–782. [CrossRef]
55. Henrichs, I.A.; O'Sullivan, G.; Chew, D.M.; Mark, C.; Babechuk, M.G.; McKenna, C.; Emo, R. The trace element and U-Pb systematics of metamorphic apatite. *Chem. Geol.* **2018**, *483*, 218–238. [CrossRef]
56. O'Sullivan, G.; Chew, D.; Mark, C.; Henrichs, I.; Morton, A. An integrated apatite geochronology and geochemistry tool for sedimentary provenance analysis. *Geochem. Geophys. Geosystems* **2018**, *19*, 1309–1326. [CrossRef]
57. Janák, M.; O'Brien, P.J.; Hurai, V.; Reutel, C. Metamorphic evolution and fluid composition of garnet-clinopyroxene amphibolites from the Tatra Mountains, Western Carpathians. *Lithos* **1996**, *39*, 57–79. [CrossRef]
58. Anczkiewicz, A.; Danišík, M.; Środoń, J. Multiple low temperature thermochronology constraints on exhumation of the Tatra Mts.—New implication for the complex evolution of the Western Carpathians in the Cenozoic. *Tectonics* **2015**, *34*, 2296–2317. [CrossRef]
59. Vrcna, S.; Štědrá, V. Crustal structure of the western part of the Bohemian Massif, Czech Republic—A summary of the project Geological model of western Bohemia, related to the deep borehole KTB in Germany. *Episodes* **1998**, *21*, 241–247.
60. Grabowski, J.; Krzemiński, L.; Nescieruk, P.; Szydło, A.; Paszkowski, M.; Pécskay, Z.; Wójtowicz, A. Geochronology of teschenitic intrusions in the Outer Western Carpathians of Poland—Constraints from 40K/40Ar ages and biostratigraphy. *Geol. Carpathica* **2003**, *54*, 385–393.
61. Lucińska-Anczkiewicz, A.; Villa, I.M.; Anczkiewicz, R.; Ślączka, A. 40Ar/39Ar dating of alkaline lamprophyres from the Polish Western Carpathians. *Geol. Carpathica* **2002**, *53*, 45–52.
62. Szopa, K.; Włodyka, R.; Chew, D. LA-ICP-MS U-Pb apatite dating of Lower Cretaceous rocks from teschenite-picrite association in the Silesian Unit (southern Poland). *Geol. Carpathica* **2014**, *65*, 273–284. [CrossRef]
63. Matýsek, D.; Jirásek, J.; Skupien, P.; Thomson, S.N. The Žermanice sill: New insights into the mineralogy, petrology, age, and origin of the teschenite association rocks in the Western Carpathians, Czech Republic. *Int. J. Earth Sci.* **2018**, *107*, 2553–2574. [CrossRef]
64. Wojewoda, J.; Migoń, P.; Krzyszkowski, D. Rozwój rzeźby i środowisk sedymentacji w młodszym trzeciorzędzie i starszym plejstocenie na obszarze środkowej części bloku przedsudeckiego: Wybrane aspekty. In *Geologia i Ochrona Środowiska Bloku Przedsudeckiego*; Przewodnik LXVI Zjazdu PTG: Wrocław, Poland, 1995; pp. 315–331. (In Polish)
65. Dyjor, S. Młodotrzeciorzędowy i eoplejstocenski rozwój sieci kopalnych dolin w Polsce na tle ewolucji paleogeograficznej obszaru bruzdy środkowopolskiej. In *Problemy Młodszego Neogenu i Eopleistocenu w Polsce*; Jahn, A., Dyjor, S., Eds.; Ossolineum: Wrocław, Poland, 1987; pp. 13–42. (In Polish)

66. Dyjor, S. Systemy kopalnych dolin Polski Zachodniej i fazy ich rozwoju w młodszym neogenie i eoplejstocenie. In *Problemy Młodszego Neogenu i Eoplejstocenu w Polsce*; Jahn, A., Dyjor, S., Eds.; Ossolineum: Wrocław, Poland, 1987; pp. 85–101. (In Polish)
67. Piwocki, M. Utwory trzeciorzędowe w okolicach Nysy. *Kwart. Geol.* **1965**, *9*, 183–192. (In Polish)
68. Walczak, W. *Pradolina Nysy i Plejstoceńskie Zmiany Hydrograficzne Przedpolu Sudetów Wschodnich*; Prace Geograficzne 2, PWN: Warszawa, Poland, 1954. (In Polish)
69. Falkowski, E. Ewolucja holoceńskiej Wisły na odcinku Zawichost-Solec i inżyniersko-geologiczna prognoza jej dalszego rozwoju. *Biul. Inst. Geol.* **1967**, *198*, 57–142. (In Polish)
70. Starkel, L. Rozwój rzeźby Polskich Karpat fliszowych w holocenie. *Pr. Geogr. Ig Pan* **1960**, *22*, 239. (In Polish)
71. Starkel, L. Last Glacial and Holocene fluvial chronology in the Carpathian valleys. *Studia Geomorphol. Carpatho-Balc.* **1977**, *11*, 33–51. (In Polish)
72. Starkel, L. Stan badań nad historią doliny Wisły w późnym glacjale i holocenie. *Przegląd Geogr.* **1981**, *53*, 3–16. (In Polish)
73. Starkel, L. The reflection of hydrologie changes in the fluvial environment of the temperate zone during the last 15,000 years. In *Background to Palaeohydrology*; Gregory, K.J., Wiley, J., Eds.; Chichester, J. Wiley and Sons: Chichester, UK, 1983; pp. 213–234.